Chapter 3
Cell Membrane: Structure and Physical Properties

The *cell membrane* (or *plasma membrane*) is a thin *closed sheet* that fulfils a double role: (a) *morphological* – delimitates the cell from its external microenvironment and confines all of its subcellular organelles; (b) *functional* – regulates the exchange of substance between internal and external media, maintains actively the ionic asymmetry between its sides, and intermediates internalization or externalization of *physical* and *chemical signals* important for cell functions.

The plasma membrane undergoes continual changes both in its molecular composition and its structure (i.e., spatial distribution of its components), although during the entire lifespan of the cell its global architecture remains the same. It plays an important role in the economy of the cell, exerting a *selective control* on the entire traffic of ions, water, and molecules.

The membrane is involved also in intake (*endocytosis*) and secretion (*exocytosis*) of large particles. For example, *macrophages*, involved in the immune defence system, are able to engulf and destroy microbes and other foreign particles, this complex cellular process being called *phagocytosis* (see chapter 4). Being placed at the exterior of a cell, the membrane is also the first target of physical, chemical, and biological agents such as thermal and mechanical stress, toxins, hormones, viruses, microbes, etc. The membrane of specialized cells, such as neurons, is involved in propagation of *nervous signals* (see chapter 6) towards other neurons in the brain or muscle and glandular cells. Finally, the plasma membrane participates actively in the process of *cellular recognition* during the complex process of *morphogenesis*, when some types of differentiated (i.e., specialized) cells are segregated to form different types of tissues.

3.1 Membrane Structure

The cell membrane has a very complex anisotropic composition and spatial structure. This allows it to perform a wide variety of general as well as specialized tasks. Although some membrane characteristics may vary from cell to cell, certain general properties are the same for every cell, as we shall see below.

3.1.1 Chemical Composition of the Plasma Membrane

The main building blocks of all membranes are: *lipids, proteins, glycoproteins, lipoproteins, water* and *ions*.

Lipid molecules are the most abundant components in the membrane. *Lipid* is a generic term which includes a broad class of molecules, the most representative being *phospholipids* and *cholesterol*. The chemical and physical properties of phospholipids have been discussed in some detail in chapter 1, in particular their amphiphilic character, which leads to their *self-association* into micelles and bilayer membranes. The molecule of cholesterol is a special type of amphiphile with a single hydrocarbon tail which induces some rigidity into a lipid bilayer and consequently, into a membrane.

Proteins are among the most important components of the cell membrane. There exists a large variety of membrane proteins (e.g., channels, carriers, ion pumps, etc.). Membrane proteins, although present in a smaller numbers than lipids, represent approximately 50% of the whole membrane mass (due to their large molecular mass). While membrane proteins could play an important role in the membrane 3D structure, they are involved especially in the membrane specific functions, as we shall see later. In fact, most of the membrane specific functions are associated with certain membrane proteins.

Glycolipids are formed, as their names suggest, by combinations between simple *sugars* and *lipids* (e.g., glucosylcerebroside, in which *glucose* is covalently attached to the lipid s*phyngosine*). Cell membranes contain 2–10% lipids complexed with different kinds of sugars.

Glycoproteins are formed by chemical interactions between membrane proteins and sugars, the latter being exposed exclusively towards the extracellular side of the membrane (such as in the case of glycophorin) forming the so-called membrane *glycocalix*.

Lipoproteins are represented by proteins chemically attached to membrane lipids, and can be found on both sides of a membrane.

Water is the solvent for all molecules in the living matter, as we have already seen in previous chapters, and it comes to no surprise that cell membranes too incorporate water molecules, either bound to the polar groups exposed on the polar side of the membrane molecules (also called "structured water") or unbound (i.e., bulk water) within pores and some ionic channels traversing the membranes from one side to another.

Ions are associated with membranes, either through simple adsorption to the two membrane surfaces or by simply transiting the membrane through ionic channels (membrane proteins) or ion pumps (membrane proteins with enzymatic character; see chapter 4). Some of the ions most often encountered in association with the membrane structure and functions are: H^+, Na^+, K^+, Cl^-, Ca^{++}, HCO_3^-.

3.1.2 Spatial Architecture of the Plasma Membrane

Over the past 70 years numerous *structural models* of the membrane have been proposed mostly based on interpretation of the complex physical properties that natural membranes exhibit. The great majority of models included as a common characteristic the existence of a *lipid bilayer*, which confers an intrinsic thermodynamic stability to the membrane. We shall skip over the intricate history of membrane model evolution over time, and shall present only the currently accepted structural model, which can explain many of the membrane properties and functions and is able to accommodate new experimental findings. This model, called the *fluid mosaic model of membrane*, was elaborated by Singer and Nicolson (1972).

According to the *fluid mosaic model*, the *basic structural frame* of the cell membrane is provided by a *lipid bilayer* in which all kinds of proteins and other complex molecules mentioned above are embedded (Fig. 3.1). According to this model, the proteins embedded in the phospholipid bilayer confer to the membrane a mosaic-like aspect, while the *fluid* character is provided by the ability of all membrane components to diffuse laterally in the bilayer "plane" (the membrane can be considered practically a 2D structure).

The main structural and physical features of the fluid mosaic model of the membrane are listed below and should be considered in conjunction with Fig. 3.1.

1. The energetic stability of the membrane structure is mainly ensured by non-covalent *hydrophilic* and *hydrophobic* interactions exerted between membrane molecules, and between them and the aqueous medium, as has been discussed in detail in chapter 1. Other types of interactions are also involved (e.g., electrostatic, hydrogen bonds, and van der Waals interactions).

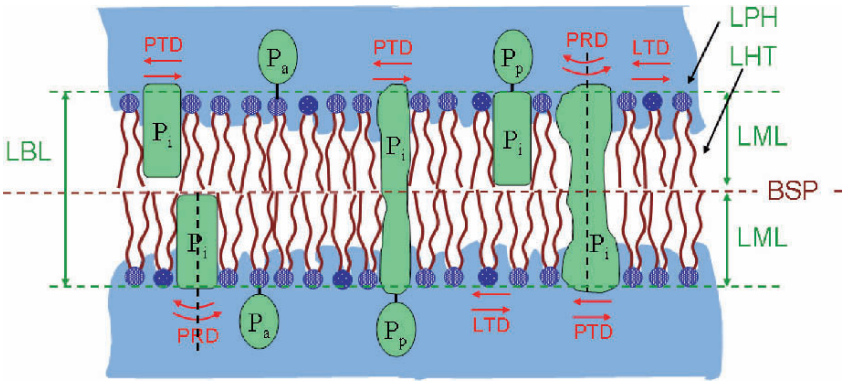

Fig. 3.1 Fluid mosaic model of the cell membrane. Significance of the symbols: LBL – lipid bilayer; LML – lipid monolayer; BSP – bilayer symmetry plane; LPH – lipid polar heads; LHT – lipid hydrophobic tails; P_i, P_p, P_a – integral, peripheral and, respectively, anchored proteins; LTD – lipid translational diffusion; PTD – protein translational diffusion; PRD – protein rotational diffusion.

2. The quasilinear lipid molecules are almost perpendicular to the membrane surfaces, so that their polar heads, involved in *hydrophilic interactions*, are facing the external and internal aqueous phases, while their tails (i.e., hydrocarbon chains) are buried inside the membrane, forming a quasiliquid *hydrophobic core* of the membrane. Generally roughly speaking, a lipid *monolayer* (also called *leaflet*) could be considered as a mirror image of the other one. (This is perfectly true only in the case of a planar bilayer composed of a single lipid species). The thickness of the plasma membrane bilayer varies from case to case between 4 and 6 nm (Berg et al., 2002). The thickness of the plasma membrane has been first estimated by Fricke (1927) from the relatively high electrical capacitance $(0.81\,\mu\mathrm{F/cm^2})$ of the plasma membrane as obtained from dielectric measurements of suspensions of cells in the audio/radio-frequency range. By assuming the permittivity of the hydrophobic layer relative to free space $(\varepsilon_0 = 8.854 \times 10^{-12}\,\mathrm{F/m})$ to be about 3, Fricke obtained a value of 3.3 nm for the thickness of the membrane, which is in good agreement with the currently accepted values, as mentioned above. More on the results of this kind of studies will be presented in sections 3.3 and 3.4.
3. The membrane components *can diffuse laterally* in the membrane plane, their diffusion coefficients (see chapter 4) depending on particles sizes and on their interactions with other particles. The translational diffusion in the membrane has been evidenced even before the fluid mosaic model was proposed, in the case of the so called hybrid "supercells" obtained by fusion of two different cell species (Frye and Edidin, 1970). The lateral (i.e., translational) diffusion, can also be easily evidenced using the technique of *fluorescence recovery after photobleaching* (FRAP) of fluorescently-labeled membrane proteins (Goodwin et al., 2005). The membrane components *can also randomly rotate* around their axes perpendicular to the membrane plane.
4. Lipid molecules can undergo *flip-flop movements*, in which they can jump from one lipid monolayer to another. These movements are energetically unfavorable and, for this transition to occur, lipids are assisted by an enzyme (*flippase*) with consumption of an ATP molecule (Lodish et al., 2004). This movement may play a role in controlling the composition in lipids of the two membrane layers.
5. Proteins associated to the membrane are of three types (Lodish et al., 2004): *integral* proteins, P_i, which are inserted into the membrane, *lipid-anchored* proteins, P_a, and *peripheral* proteins, P_p, which are weakly bound to the membrane (Fig. 3.1).

   Integral proteins can be either transmembranar, crossing the membrane from one face to another (e.g., the channels, carriers and ionic pumps) or may be embedded more or less into only one monolayer. There exist integral proteins that cross the bilayer only once (e.g., glycophorin A) (Lodish et al., 2004; Berg et al., 2002), or several times. For instance the K^+ channel (see chapter 7) crosses the bilayer two times, while the mammalian glucose transporter crosses the bilayer twelve times (Fig. 3.2). In all these cases, the intramembrane strands are organized as α-helices, but there are also proteins (e.g., porins) that are organized only

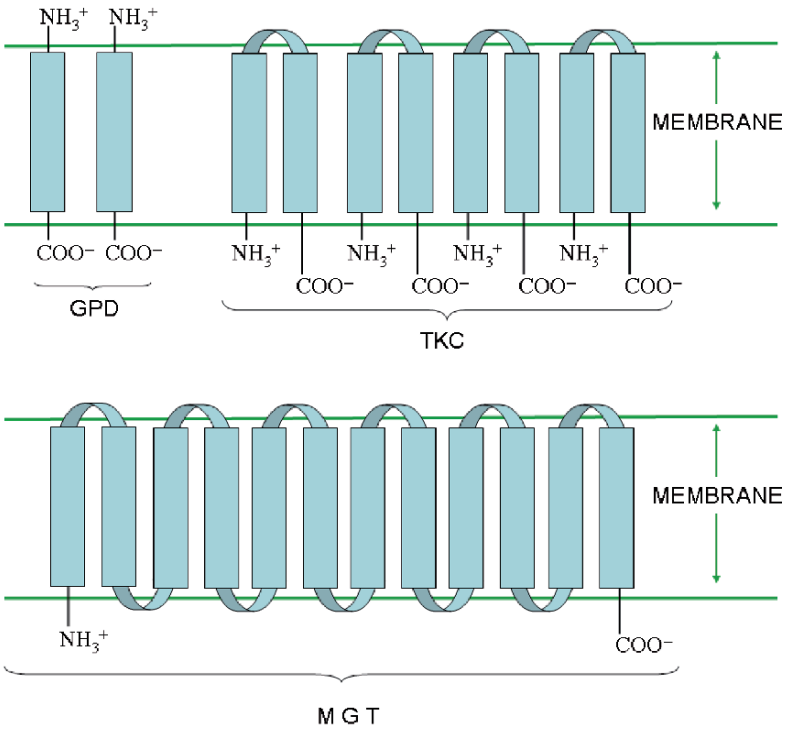

Fig. 3.2 Various kinds of spatial relations between integral proteins and the bilayer frame. Significance of the symbols: GPD – Glycophorin dimer; TKC – tetrameric potassium channel; MGT – Mammalian glucose transporter.

as β-strands and are able to traverse many times the lipid bilayer, forming, in the case of bacteria (e.g., *Escherichia coli*), membrane channels for disaccharides, phosphates and other small molecules. The segments of the integral proteins embedded in the membrane are composed especially of hydrophobic amino acids, while their parts exposed out of the lipid bilayers are predominantly formed from hydrophilic amino acids.

Peripheral proteins can be easily removed from the membrane. They are very important in the economy of the cell, for ensuring the transmission of many specific signals, either from the exterior to the interior of the cell or conversely, *via* the integral proteins.

6. There is always a non-uniform distribution of proteins and protein-complexes among the two phospholipids monolayers, which leads to an *asymmetry* of the membrane. For instance, *glycoproteins* are only associated with *the outer monolayer*, forming the so called cellular *glycocalix*, while in the particular case of erythrocytes, a peripheral protein called *spectrin* is associated only to the *internal face* of the membrane. Moreover, integral proteins are always exposing on

the two membrane surfaces different portions of their strands, thereby contributing to the structural asymmetry of the membrane. Unlike lipids, proteins do not undergo flip-flop motion, the asymmetric protein distribution being permanently maintained in the membrane.

7. Due to the thermal motions of lipids, some pores could appear transiently at random positions in the lipid matrix of the double layer, permitting a direct communication between the interior and exterior of the cell (Popescu et al., 2003; Movileanu et al., 2006). Due to the hydrophilic and hydrophobic interactions, these pores are rapidly resealed.

In conclusion, the cell membrane is a complex and dynamic structure which accomplishes essential functions in the cell, as we shall see later, in next chapters.

3.2 Surface Charges

3.2.1 Origin of the Surface Charges

When microscopic or macroscopic objects are immersed in an aqueous electrolyte solution, their surfaces become *electrical charged*, except for the particular case of the so-called *isoelectric pH*, when their net surface charge is zero. The electrical charge is due to the *adsorption* of anions and cations onto the body surfaces. As we have seen in chapter 1, both types of ions are hydrated, but the cations have a thicker hydration shell. As a result of this, the cation charges are more screened than those of anions and their interaction with the immersed surfaces is weaker. This leads to a preferential adsorption of anions as compared with cations. Alternatively, one can say that the anions present greater *polarizabilities* and, consequently, are better adsorbed. This mechanism of electrical charging of the surface is called *extrinsic charging mechanism*, being induced by the immersion medium.

Observation: If the solution pH is decreased, the surface charges are strongly modified, on one hand, due to H^+ electrostatic interaction with already adsorbed anions and, on the other hand, due to direct H^+ adsorption onto the surface. Thus, beyond the isoelectric pH the surface charge changes its sign. It is important to note that H^+ is more easily adsorbed onto neutral sites of a membrane surface, being associated only with one water molecule (i.e., forming the so called *hydronium* ion: H_3O^+).

In the case of biological membranes, besides the extrinsic charging mechanism, an *intrinsic charging mechanism* is also acting, due to the electrical *dissociation* of the chemical groups on the membrane surface. Thus, at neutral pH, which characterizes the great majority of biological liquids, most of the dissociable chemical groups generate mainly negative charges. For instance, the phospholipid head groups can dissociate to generate $–H_2PO_4^-$, $–HPO_4^{-2}$, $–PO_4^{-3}$, while the sialic acid associated with integral proteins generates $–COO^-$ groups. It is also possible for some amino groups to become positively charged ($–NH_3^+$). However, in physiological

solutions, the contribution of the positive groups is overwhelmed by that of the negative groups, so that the *intrinsic mechanism* too leads to a net negative surface charge. This is supported by the experimental evidence that cells migrate towards the *anode* when subjected to an external electrical field.

Observation: Although the net surface charge of biological surfaces is negative, there may be patches on the cell surface that are positively charged. Therefore one can speak of a mosaic of electrical charges on the cell membranes both concerning their nature and their charge signs. These surface charges form a *dynamic electrostatic landscape* with an irregular pattern.

3.2.2 Electrical Double Layer

Electrical charges on the surface of biological particles exert an antientropic effect (i.e., $\Delta S_a < 0$) on the populations of ions located in the vicinity of the surface. This leads to a tendency to organize the nearby charges spatially, the *counter-ions* (i.e., ions with opposite charge to surface) being electrostatically attracted, and the *co-ions* (i.e., ions with same sign as the surface) being repelled. As a consequence, the surface charges lead to generation of an *electrical double layer*, which roughly consists of a layer of charges pertaining to the surface, and a layer of counter-ions at a small distance.

By contrast to the antientropic effect of the surface charges, thermal agitation of the ions has an entropic effect ($\Delta S_e > 0$), disrupting the organization of the surface charges, affecting thus the structure of the double layer (compared to what it would be, for instance, at very low temperatures).

Due to these two opposite tendencies, a "tradeoff structure" of the ion populations near the surface is attained, in which the organizing effect of the surface charges prevails near the surface (i.e., $\Delta S_a + \Delta S_e < 0$), while leading to an overall increase in entropy in the bulk solution ($\Delta S_b > 0$). With this, the second law of thermodynamics is obeyed, because $\Delta S_a + \Delta S_e + \Delta S_b > 0$.

The tradeoff electrical double layer has two components (Fig. 3.3): a *compact* or *Helmholtz double layer* (CDL) (Glaser, 2001), whose counter-ion charges do not completely neutralize the surface charges, and a *diffuse double layer* (DDL), whose counter-ion charges neutralize the charges left uncompensated by the CDL. Within DDL, the counter-ions concentration decreases with distance from the surface, while the concentration of co-ions increases. The specific dependence of ion concentrations on distance will be derived below.

3.2.3 Gouy-Chapman-Stern Theory of the Electrical Double Layer

Gouy (1910) and Chapman (1913) independently developed a diffuse double layer model in which ions are free to move (Brett and Oliveira Brett, 1993). In 1924, Stern combined the Helmholtz model for CDL, with the Gouy-Chapman model for DDL

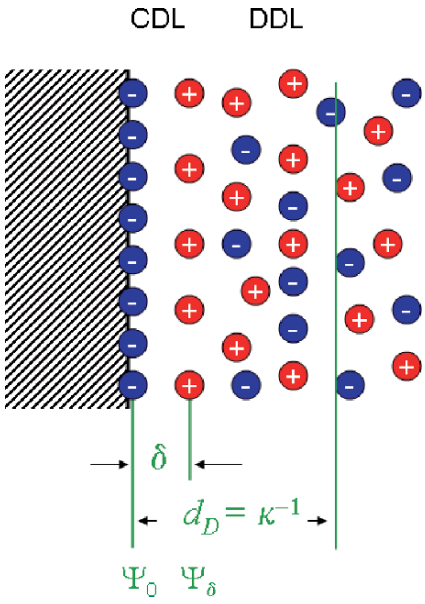

Fig. 3.3 Schematic representation of an electrical double layer near a planar surface of a solid particle (hatched). CDL – Helmholtz compact double layer; DDL – diffuse double layer; δ – compact layer thickness; d_D – Debye length, Ψ_0 – surface potential; Ψ_δ – Stern potential (see text for the physical meaning of the parameters).

(Atkins and de Paula, 2002). Later, in 1947, Grahame developed a more complex model, considering also the specifically adsorbed ions onto the solid surface (Brett and Oliveira Brett, 1993).

3.2.3.1 Problem Formulation and Simplifications

In the case of smooth surfaces, the geometry of the double layer is rather simple: if the surface has a planar or curved shape the double layer will have a planar or curved shape too. By contrast, most biological particles present irregular surfaces, which lead to electrical double layers with very complicated geometrical shapes that lead to very elaborated mathematical models. For this reason, and for many other reasons that will become clearer as we proceed with the mathematical treatment of the double layer, we will make the following simplifying assumptions:

(a) For spheroidal particles (such as cells), the radii of the hydrated ions are much smaller then the local radius of curvature of the surface (i.e., a few Ångstroms vs. $>5\,\mu m$); therefore, the ions are considered as *point charges*.
(b) The double layer is located near the cell surface.
(c) The surface charges are assumed to be distributed uniformly over the cell surfaces. The lipid bilayer fluidity has the tendency to lead to uniform distribution of the electrical charges on the surface, while the cytoskeleton has the opposite tendency.
(d) Partly due to approximation (a), the mathematical treatment can be applied to a very small area of the particle surface, so that even for spherical particles a planar model will provide a good approximation. From an electrical point of view,

this amounts to assuming that the *electrical potential* to the "left" (Fig. 3.3) of the double layer and *inside the spherical particle is constant*. This assumption greatly simplifies the mathematical treatment of the physical model.

In addition to the geometrical simplifications suggested above, we shall also make some assumptions concerning the electrolyte composition (less drastic than the ones above). The aqueous medium is electrically neutral, and is composed of p kinds of ions (both, anions and cations) of electrovalence, z_k $(k = 1, 2, \ldots, p)$, having very low concentrations (so that the solution could be considered dilute). An infinitesimal volume, dV, centered on a point, P, located inside the double layer has a partial net charge, $dq_k = z_k e\ dN_k$, where dN_k is the number of ions of species k contained in dV. We can now express the partial electrical charge density, ρ_k, of the element of volume dV as:

$$\rho_k(P) = \frac{dq_k}{dV} = n_k(P) z_k e, \tag{3.1}$$

where $n_k = dN_k / dV$ represents the numeric concentration of the ionic species k (i.e., the number of ions of the unit volume). The total charge density, $\rho(P)$, at a point, P, is given by the sum of each ion contribution:

$$\rho(P) = \sum_{k=1}^{p} n_k(P) z_k e. \tag{3.2a}$$

Since, according to the approximations above, the double layer may be considered planar, the charge density at any point contained in a plane parallel to the particle surface and situated at the distance, x, from the surface will be always the same. This means that the mathematical description of the double layer can be reduced to a single spatial dimension, x. Thus the total charge density, at a distance, x, is given by the sum of over all ion contributions:

$$\rho(x) = \sum_{k=1}^{p} n_k(x) z_k e. \tag{3.2b}$$

3.2.3.2 Poisson-Boltzmann Equation and the Electrical Potential

Having defined the volume charge density, we can now relate the electrical potential, Ψ, at any point in the double layer, to the charge density, according to the *Poisson equation*:

$$\Delta\Psi(x) = -\rho(x)/\varepsilon, \tag{3.3}$$

where Δ $(= \nabla^2)$ is the second order differential *Laplacean operator*, and ε is the permittivity of the medium.

Observation: The permittivity varies with the distance from the double layer. However, the exact form of its variation is usually unknown, so one has to make certain approximations, as we shall see below.

By combining equations (3.2b) and (3.3) and writing explicitly the one-dimensional character of our problem, we obtain:

$$\frac{d^2\Psi(x)}{dx^2} = -\frac{e}{\varepsilon}\sum_{k=1}^{p} n_k(x) z_k. \tag{3.4}$$

In order to solve the Poisson equation, we need to know how n_k varies with distance. In the Gouy-Chapman theory, it is assumed that the energetic states of each ion, k, are described by a Boltzmann distribution, given the thermal equilibrium that is normally attained by the ion populations. Therefore, one can write:

$$n_k(x) = n_k(\infty)\exp\left[-\frac{z_k e\Psi(x)}{k_B T}\right] \tag{3.5}$$

where $n_k(\infty)$ represents the concentration of k ionic species in the bulk solution (i.e., at $x \to \infty$) and k_B is the Boltzmann constant.

Combining equations (3.4) and (3.5), one obtains the so-called *Poisson-Boltzmann equation* of the planar double layer:

$$\frac{d^2\Psi(x)}{dx^2} = -\frac{e}{\varepsilon}\sum_{k=1}^{p} z_k n_k(\infty)\exp\left[-\frac{z_k e\Psi(x)}{k_B T}\right], \tag{3.6}$$

which is a nonlinear differential equation that could be only numerically solved.

However, by making further approximations, equation (3.6) can be analytically solved. Indeed, if we assume that the electrical potential at the particle surface, $\Psi(0) = \Psi_0$, is less than about 25 mV, the exponent in equation (3.6) is smaller than 0.01. Therefore, we can expand (3.6) in Taylor series around $x = 0$ and retain only the first order term, to obtain:

$$\frac{d^2\Psi(x)}{dx^2} \cong -\frac{e}{\varepsilon}\sum_{k=1}^{p} z_k n_k(\infty)\left[1 - \frac{z_k e\Psi(x)}{k_B T}\right]. \tag{3.7}$$

In this expression, the first part of the sum is $\sum_{k=1}^{p} e z_k n_k(\infty) = \rho(\infty) = 0$, because of the neutrality of the solution. With this, equation (3.7) further simplifies to:

$$\frac{d^2\Psi(x)}{dx^2} \cong \kappa^2\,\Psi(x), \tag{3.8}$$

where we have introduced the customary notation:

$$\kappa = \left[\frac{e^2}{\varepsilon k_B T}\sum_{k=1}^{p} z_k^2 n_k(\infty)\right]^{\frac{1}{2}}. \tag{3.9}$$

Here, κ represents the *Debye-Hückel parameter*, which depends on the physical properties of the electrolyte, and is independent of the nature of the particle surface.

For the moment, we shall limit ourselves to stating that the Debye-Hückel parameter depends on the square root of the *ionic strength, I*, of the electrolyte solution, given by:

$$I = \frac{1}{2}\sum_{k=1}^{p} z_k^2 c_k(\infty) = \frac{1}{2N_A}\sum_{k=1}^{p} z_k^2 n_k(\infty), \tag{3.10}$$

where $c_k(\infty)$ is the molar concentration of the k species, that is, $c_k(\infty) = n_k(\infty)/N_A$ (N_A being Avogadro's number).

Observation: The ionic strength, I, depends on the second power of the electrovalences, z_k. Therefore two solutions with same concentration can present quite different ionic strengths and thus can have quite different influences on the surface charge screening. Indeed, if a solution contains, e.g., Al^{3+} and another contains Na^{+}, the contribution of the trivalent ions to the sum (3.10) will be nine times greater than that of monovalent sodium ions.

By using equation (3.10), equation (3.9) becomes:

$$\kappa = \left[\frac{2e^2 N_A}{\varepsilon k_B T} I\right]^{\frac{1}{2}} = \left[\frac{2F^2}{\varepsilon RT} I\right]^{\frac{1}{2}}, \tag{3.11}$$

where the following relations have been used: $eN_A = F$ (Faraday's number) and $k_B = R/N_A$.

For x ranging over the interval (0, δ), there are no electrical charges, and the Poisson-Boltzmann equation (3.8) reduces itself to the *Laplace equation*, which can be solved by successive integrations to give:

$$\Psi(x) = ax + b, \tag{3.12}$$

where a and b are two constants that can be determined from the boundary conditions at $x \to 0$ (which gives $b = \Psi_0$) and $x \to \delta$ $\left(\text{giving } a = (\Psi_\delta - \Psi_0)/\delta\right)$. Thus,

$$\Psi(0 < x < \delta) = \frac{\Psi_\delta - \Psi_0}{\delta} x + \Psi_0, \tag{3.13}$$

and therefore in the *Stern space*, $0 < x < \delta$, the absolute value of electrical potential *decreases linearly* with the distance from the charged surface.

The general solution of equation (3.8) for $x \in [\delta, \infty)$ is:

$$\Psi(x) = A\exp(-\kappa x) + B\exp(+\kappa x). \tag{3.14}$$

By imposing the following boundary conditions $\Psi(x \to \delta) = \Psi_\delta$ (*Stern potential*) and $\Psi(x \to \infty) = 0$ (that is, far enough from the surface, the potential vanishes, due to electroneutrality of the medium), it results $B = 0$, so that the particular solution of the equation (3.14), having a physical meaning, is of the form:

$$\Psi(x \geq \delta) = \Psi_\delta \exp\left[-\kappa(x - \delta)\right]. \tag{3.15}$$

Therefore, the absolute value of the electrical potential *decreases exponentially* with the distance for $x \geq \delta$. This means that the electrical potential generated by the

surface charges is screened by the counter ionic atmosphere. Moreover, this screening depends on the ionic strength, which is included in κ (Debye-Hückel parameter) through equation (3.11), the solutions with a greater ionic strength being more effective in charge screening.

At this point, we can discuss the physical meaning of the Debye-Hückel parameter. By convention, because the DDL has no precise boundaries, the "thickness" of the DDL is defined as the distance, d_D, at which the electrical potential decreases by e (e being the base of the natural logarithm, or the *Euler number*) as compared to Ψ_δ, namely

$$\Psi(d_D) = \Psi_\delta e^{-\kappa(d_D-\delta)} = \Psi_\delta/e. \tag{3.16}$$

Thus, $1/\kappa = d_D - \delta \approx d_D(\delta \ll d_D)$, that is, the *reciprocal* of *Debye-Hückel parameter* is equal with the *thickness* of the *diffuse double layer* (Figs. 3.3 and 3.5) and called *Debye length*.

The Debye length is a measure of how far the effect of surface charges may be felt into the bulk of the solution. It depends on the ionic strength of the solution. Thus, in Ringer solution (a solution of salts in water that prolongs the survival time of excised tissue), the Debye length is 7.8 Å (Hille, 2001), while in physiological saline (i.e., 0.145 M NaCl) it is 8 Å.

Therefore the effect of surface charges on the ions in physiological solutions extends into the double layer over distances much shorter than the size of the macromolecules (Hille, 2001).

Observation: In the case of the natural plasma membrane, the Stern layer (Fig. 3.3) is also populated with ions entering into or exiting from the membrane (due to membrane permeability to ions), and relation (3.16) does not hold any more.

Quiz 1. Plot the Debye length as a function of concentration for solutions of NaCl having the following concentrations: (a) 1 µM; (b) 10 µM; (c) 100 µM; (d) 1 mM; (e) 10 mM; (f) 100 mM.

3.2.3.3 Measuring the Electrochemical Potential Through Electromigration

Particles migrating through an aqueous milieu carry along an ionic shell of thickness a. The sum of the particle radius and the shell thickness is referred to as the *electrokinetic radius*, r_{ek}. The surface of separation, at $x = a$, between the moving and non moving part of the charge cloud is called the "slipping plane" or shear plane (Fig. 3.4).

Depending on their surface charges, biological particles (cells, organelles, viruses, etc.) suspended in physiological solutions can migrate in an electrical field, E, with different *mobilities*, u, defined as:

$$u = v/E \tag{3.17}$$

where v is the relative velocity of the particle driven by the electrical field. This phenomenon of migration of electrically charged particles in an electrical field is called

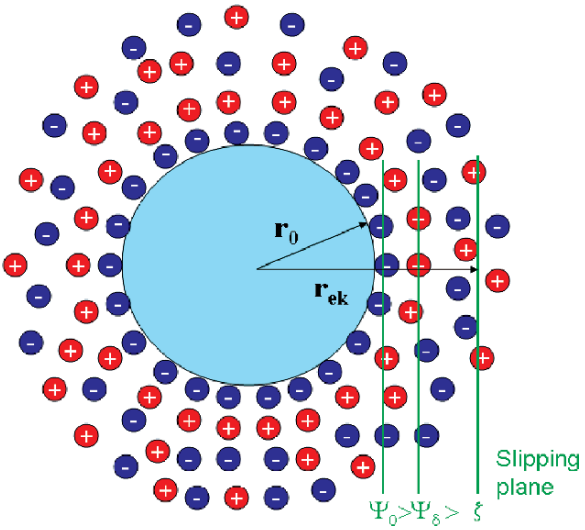

Fig. 3.4 Geometrical and electrokinetic radii of an electrically charged particle. The potential measured in the slipping plane is called the *zeta* potential (ζ), and can be determined experimentally from measurements of electrokinetic mobility, i.e., from electrophoresis (see text below); r_0 is the particle radius; r_{ek} is the effective radius of the particle including part of the counterion cloud.

electrophoresis and has practical applications in biophysics and colloidal chemistry, as we will discuss briefly below.

Figure 3.5 shows an example of variation of electrical potential with distance from the charged surface, as predicted by a combination of equations (3.13) and (3.15). Generally, one can find the following relation among the three defined potentials:

$$|\zeta| < |\Psi_\delta| < |\Psi_0| \,. \tag{3.18}$$

The electrical potential, at the distance $x = \delta$ (i.e., at the slipping plane) is called *electrokinetic potential* or *zeta potential*, $\Psi(\delta) = \zeta$, while the other potentials have been defined in the discussion above. The zeta potential is the only potential related to the electrical double layer that can be measured directly (by electrophoresis), and as such, it provides an indication of the order of magnitude of the other potentials.

In the case of spherical particles of geometrical radius, r_0, the *most general theory* giving mathematical relation between ζ and u (electrophoretic mobility), is due to *Henry*.

According to the *Henry theory* (Hunter, 1987), the relation is:

$$u_{HR} = \frac{2}{3}\frac{\varepsilon\zeta}{\eta} f(\kappa r_0) \tag{3.19}$$

where ε represents the dielectric constant of the solution, η is its dynamical viscosity coefficient, and $f(\kappa r_0)$ is the empirical Henry function, taking values over the range [1, 3/2], for $\zeta < 25\,\text{mV}$.

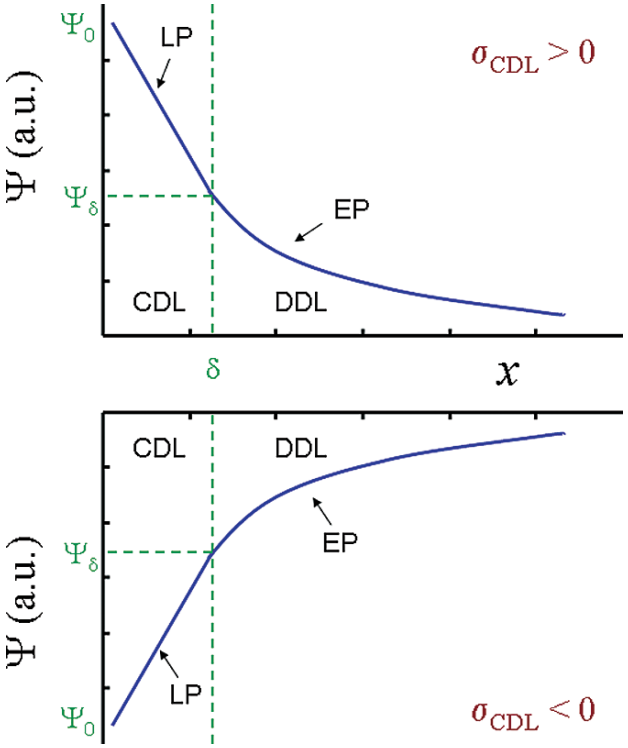

Fig. 3.5 Dependence of electrical potential in the double layer on the distance x from the surface for positive (top panel) and negative (bottom) charge density of the compact double layer. Significance of the symbols: CDL – compact double layer; DDL – diffuse double layer; SP – Stern plane; SS – slipping plane; Ψ_0 – surface electrical potential; Ψ_δ – Stern electrical potential; LP, EP – linear and respectively, exponential portion of the potential's spatial dependence.

For the largest biological particles suspended in relatively dilute electrolyte (i.e., cells), $\kappa r_0 > 100$. In this situation, $f(\kappa r_0) = 3/2$, and (3.19) reduces to the simpler *Helmhlotz-Smoluchowski* formula:

$$u_{HS} = \frac{\varepsilon \zeta}{\eta}. \tag{3.20}$$

In the opposite case when *smaller biological particles* are taken into account (e.g., viruses), $\kappa r_0 < 0.1$, and $f(\kappa r_0) = 1$, and (3.19) reduces to the *Hückel* formula:

$$u_{HK} = \frac{2}{3}\frac{\varepsilon \zeta}{\eta}. \tag{3.21}$$

For the intermediate cases, $0.1 < \kappa r_0 < 100$, one must employ the more general *Henry* formula.

Observation: The electrical double layer around biological particles is also involved in the electrostatic interaction between cells suspended in a physiological solution.

Practically, the mobility of single cells subjected to external electrical fields can be determined under an optical microscope; the technique is called *micro-electrophoresis* and can be used for determination of the zeta potential.

Electromigration of ultra-small biological particles is used widely in biological and biochemical laboratories for separation and identification of fluorescently stained macromolecules or fragments of macromolecules, such as for DNA fragment identification in gel-electrophoresis.

3.2.3.4 Surface Charge Density and the Electrical Capacitance of the Double Layer

In this section, we will derive a simple relationship between a specific electrical capacitance of the electrical double layer and the Debye length, thereby providing a means for determining the later. We begin by writing the surface charge density of the diffuse layer as the line integral of the total volume charge of the counter ion layer, namely:

$$\sigma_{DDL} = \sum_k \int_\delta^\infty z_k e n_k(x)\, dx = \int_\delta^\infty \rho(x) dx. \tag{3.22}$$

The integral can be also obtained by integrating the Poisson equation (3.3). Thus:

$$\sigma_{DDL} = -\varepsilon_{DDL} \int_\delta^\infty \frac{d^2\Psi}{dx^2} dx = -\varepsilon_{DDL} \left.\frac{d\Psi}{dx}\right|_\delta^\infty = -\varepsilon_{DDL} \left(0 - \left.\frac{d\Psi}{dx}\right|_\delta\right). \tag{3.23}$$

From (3.15), $\dfrac{d\Psi}{dx} = -\kappa\Psi_\delta \exp[-\kappa(x-\delta)]$, and therefore:

$$\sigma_{DDL} = -\varepsilon_{DDL}\kappa\Psi_\delta. \tag{3.24}$$

Similarly, for the singularity at $x = 0$ (i.e., the fixed surface charge), we obtain:

$$\sigma_{CDL} = -\varepsilon_{CDL}\frac{\Psi_\delta - \Psi_0}{\delta}, \tag{3.25}$$

where we have used the approximation (d) in section 3.2.3.1, to set the potential at $x = 0$ equal to a constant, Ψ_0. This approximation is also valid for a planar lipid bilayer with symmetrical electrical double layers.

Since $\sigma_{DDL} = -\sigma_{CDL}$ (due to electroneutrality of the system), we get:

$$\Psi_\delta = \Psi_0 \frac{\varepsilon_{CDL}}{\varepsilon_{CDL} + \varepsilon_{DDL}\kappa\delta} = \frac{\Psi_0}{1 + \frac{\varepsilon_{DDL}}{\varepsilon_{CDL}}\kappa\delta}. \tag{3.26}$$

For small concentrations ($c \to 0$, i.e., weak electrolytes) or, equivalently, $\kappa\delta \ll 1$, equation (3.26) gives $\Psi_\delta \approx \Psi_0$. The charges on the Stern layer are compensated only at large distances from the surface. On the other hand, if the concentration is large (i.e., strong electrolytes), we have $\kappa\delta \gg 1$, and equation (3.26) gives $|\Psi_\delta| \ll |\Psi_0|$. In this case, the Stern layer almost completely neutralizes the adsorbed charges.

By using equations (3.24) and (3.26), we can now determine the specific electrical capacitance (i.e., capacitance divided by the surface area) of the electrical double layer, simply as the ratio between the surface charge density and the potential difference detected between an electrode placed at $x = 0$ and another one for $x \to \infty$, namely:

$$C_{DL} = \frac{\sigma_{DDL}}{\underbrace{\Psi(\infty)}_{0} - \Psi_0} = \frac{-\varepsilon_{DDL}\kappa\Psi_\delta}{-\Psi_0} = \frac{\varepsilon_{DDL}\kappa}{1 + \frac{\varepsilon_{DDL}}{\varepsilon_{CDL}}\kappa\delta}. \tag{3.27}$$

As we mentioned in the preceding sections of this chapter, in general, the permittivity varies with the distance from the particle surface and into the bulk of the electrolyte in a manner unspecified. We will take this variation into account by distinguishing between the three main layers, namely $\varepsilon_{CDL} < \varepsilon_{DDL} < \varepsilon_{water}$.

For small concentrations, $c \to 0$ and $C_{DL} \to \varepsilon_{DDL}\kappa$. If we consider, for example, a 10 mM KCl solution, and $\varepsilon_{DDL} \approx 30\varepsilon_0$, we obtain a capacitance of the double layer $C_{DL} \approx 100\,\mu\text{F/cm}^2$. Conversely, this capacitance can be determined from electrical measurements on lipid bilayers, and the Debye length can thus be determined experimentally. We will discuss methods for measuring electrical capacitances of membranes in the next sub-section.

3.3 Static Electrical Properties of Planar Membranes

As it was mentioned in section 3.1, the thickness of the plasma membrane has been determined indirectly from measurements of permittivity and conductivity of cell suspensions subjected to alternating fields in the audio/radiofrequency range (Fricke, 1927). This method, generically known as *dielectric* or *impedance spectroscopy*, has since been applied to the study of electrical properties of artificial as well as natural membrane bilayers. By selecting the range of frequencies of the applied field, one can obtain information about different layers of the cell membrane as well as of other membranes internal to the cell. In this section, we will introduce the reader to the principles of the *dielectric spectroscopy method* and will discuss its application to the determination of the dielectric properties of the main layers (electrical double layer, the polar head region, and the hydrophobic core) of artificial lipid bilayers, as well as of the plasma membrane of the cell. The main goal will be to illustrate that, in spite of the difficulties one faces in trying to directly observe the plasma membrane, there are very good reasons to believe that the membrane model introduced in section 3.1, which considers that the membrane consists of a lipid-bilayer matrix, is correct.

3.3.1 Electrical Parameters as Complex Quantities

Throughout section 3.3, we will employ the concepts of *complex permittivity* and *complex conductivity*, which will be defined momentarily.

To begin with, let us define an "alternating" electric field, $E(t)$, as

$$E(t) = E_0 e^{j\omega t} \tag{3.28}$$

where E_0 is the constant part (amplitude) of the field, $\omega (= 2\pi f$ with f being the frequency) is the angular frequency of the field and $j = \sqrt{-1}$.

The general expression for an electrical current density $[J = I/(Surfacearea)]$ is given by the Ohm law for variable fields,

$$J(t) = \sigma E(t) + \frac{\partial D(t)}{\partial t} \tag{3.29}$$

where D is electrical displacement ($= \varepsilon\, E$ with ε the *permittivity*).

The above equation suggests that the *conductivity*, σ, is related to instantaneous motion of charges (either translation of rotation), while the *permittivity*, ε, is related to a delay in the particle response to the applied field.

For a constant permittivity, equations (3.28) and (3.29) give:

$$J = (\sigma + j\omega\varepsilon) E \stackrel{def}{=} \sigma^* E \tag{3.30}$$

where we have introduced the notation, σ^*, which represents the *complex conductivity*. It is also possible to introduce a quantity called *complex permittivity*, defined by the following relations:

$$\varepsilon^* \stackrel{def}{=} \frac{\sigma^*}{j\omega} = \varepsilon - j\frac{\sigma}{\omega} \stackrel{def}{=} \varepsilon - j\varepsilon'. \tag{3.31}$$

Both σ^* and ε^* are very useful in the theory of dielectrics, because they offer a synthetic way of dealing with the true permittivity and conductivity at the same time.

Materials characterized both by permittivity and conductivity (i.e., present both free and bound charges) are generically referred to as dielectrics.

Let us assume that such a dielectric material is placed between the plates of a parallel-plate capacitor and subjected to a voltage U. A quantity, called admittance, Y, will be measured, which relates to the complex conductivity through:

$$Y \stackrel{def}{=} \frac{I}{U} = \frac{JS}{Ed} = \sigma^* \frac{S}{d}, \tag{3.32}$$

where S is the surface area of each of the two identical plates, and d is the separation between them. Y is a complex number and can be rewritten, by taking equation (3.30) into account, as:

$$Y = \sigma \frac{S}{d} + j\omega\varepsilon \frac{S}{d} = G + j\omega C, \tag{3.33}$$

where G represents the *conductance* and C the *capacitance* of the dielectric material. Equation (3.33) corresponds to a parallel combination of a conductance, G, with a capacitance, C. One can also define the inverse of the admittance or the *impedance*:

$$Z \overset{def}{=} \frac{1}{Y} = \frac{1}{G + j\omega C}. \tag{3.34}$$

Observation: If a system consists of a series combination of two admittances Y_1 and Y_2, the equivalent admittance is:

$$\frac{1}{Y} = \frac{U_1 + U_2}{I} = \frac{1}{Y_1} + \frac{1}{Y_2}, \text{ or } Z = Z_1 + Z_2 \tag{3.35}$$

where U_1 and U_2 are two potential differences applied to each circuit of admittance Y_1 and Y_2, respectively. If $C_1 = 0$ and $G_2 = 0$, equation (3.34) gives:

$$Z = \frac{1}{G_1} + \frac{1}{j\omega C_2} = R_1 + \frac{1}{j\omega C_2} \tag{3.36}$$

which upon a re-notation gives the definition of the impedance for a *series combination* of a resistor and a capacitor,

$$Z = R + \frac{1}{j\omega C}. \tag{3.37}$$

3.3.2 Dielectric Relaxation of a Dielectric Multi-Layer

3.3.2.1 Interfacial Maxwell-Wagner Polarization

Let us consider a system formed of two stacked dielectric layers "sandwiched" between the plates of a parallel-plate capacitor. Each of the two layers (Fig. 3.6) can be represented by a parallel combination of capacitance and conductance (i.e., complex permittivity multiplied by a geometrical factor – see equation (3.33), for the case of a parallel-plate capacitor).

The measured admittance of the circuit is:

$$Y = \left[1/(G_1 + j\omega C_1) + 1/(G_2 + j\omega C_2)\right]^{-1}. \tag{3.38}$$

Rearranging the right-hand side of this equation, one obtains (Hanai, 1960):

$$C^* = C_h + \frac{C_l - C_h}{1 + j\omega\tau} - j\frac{G_l}{\omega}, \tag{3.39}$$

where the following convenient notations have been introduced:

$$C_h = \frac{C_1 C_2}{C_1 + C_2},$$

$$C_l = \frac{C_1 G_2^2 + C_2 G_1^2}{(G_1 + G_2)^2},$$

$$\tau = \frac{C_1 + C_2}{G_1 + G_2},$$

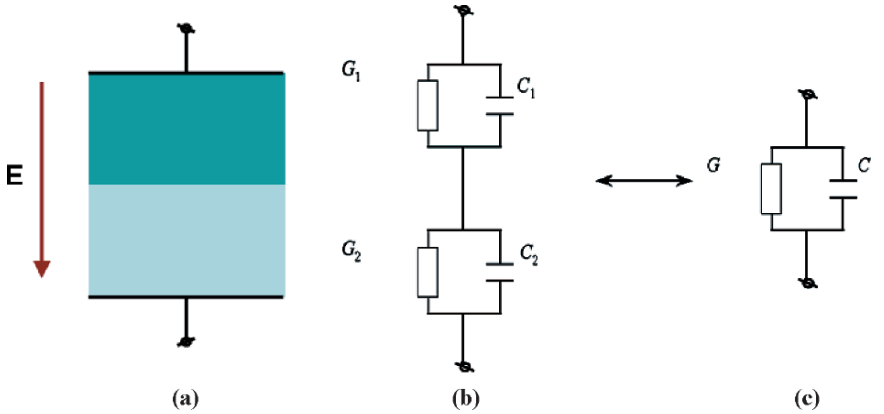

Fig. 3.6 Two stacked dielectrics placed between the plates of a parallel-plate capacitor (**a**), each being characterized by an electrical capacitance C_i and a conductance G_i ($i = 1,\ 2$) (**b**), present an equivalent capacitance C and conductance G (**c**), which are both frequency dependent, as described in the text.

(a parameter that has dimension of time), and

$$G_h = \frac{G_1 G_2}{G_1 + G_2}.$$

Further, if we divide the whole relationship (3.39) by the geometrical factor, S/d, to return to complex permittivity, we get the Debye dispersion function (Debye, 1945; Takashima, 1989),

$$\varepsilon^* = \varepsilon_h + \frac{\varepsilon_l - \varepsilon_h}{1 + j\omega\tau} - j\frac{\sigma_l}{\omega}, \tag{3.40}$$

where τ is the *relaxation time*, ε_l and σ_l are the *limiting permittivity* and *conductivity at low frequencies* (i.e., for $\omega \to 0$), ε_h and σ_h the *limiting permittivity* and *conductivity at high frequencies* (i.e., for $\omega \to \infty$) and $\varepsilon_l - \varepsilon_h = \delta\varepsilon$ is called the *dielectric increment*.

> **Observation:** A *conductivity increment*, $\sigma_l - \sigma_h = \delta\sigma$, can also be defined, but it is rarely used in practice.

By defining τ in terms of a *characteristic frequency*, f_c ($= 1/2\pi\tau$), and using the frequency f instead of the angular frequency ω, we can re-write equation (3.40) as:

$$\varepsilon^* = \varepsilon_h + \frac{\varepsilon_l - \varepsilon_h}{1 + jf/f_c} - j\frac{\sigma_l}{2\pi f}. \tag{3.41}$$

Finally, by using the Kramers-Krönig relationship between $\delta\varepsilon$ and $\delta\sigma$, which for the Debye case takes the simple form (Hanai, 1960; Takashima, 1989) $\delta\varepsilon = \tau \cdot \delta\sigma$, we obtain

$$\varepsilon = \varepsilon_h + \frac{\varepsilon_l - \varepsilon_h}{1 + \left(f/f_c\right)^2}, \tag{3.42}$$

for the real part of the equation (3.41), and

$$\sigma = \sigma_l + \frac{\sigma_h - \sigma_l}{1 + \left(f/f_c\right)^2} \cdot \left(f/f_c\right)^2, \tag{3.43}$$

for the imaginary part. These two quantities represent the *equivalent permittivity* and the *equivalent conductivity*, respectively, of the stack of two dielectric layers, and both depend on the frequency of the applied field as shown in Fig. 3.7. This frequency dependence is called dielectric dispersion.

Interestingly, a system formed by two dielectric layers stacked together behaves similarly to a pure system of permanent dipoles placed in an alternating electrical field, for which Debye equation has actually been derived initially. The role of electrical dipoles is played in this case by the accumulation of electrical charges at the interface between the two dielectric layers; the frequency dependence arises from the fact that the magnitude of the charge falls off with the increase in the frequency of the applied field. The mechanism of dielectric dispersion is known in the literature on dielectric spectroscopy as *Maxwell-Wagner interfacial polarization* or simply as *interfacial polarization*.

More insight can be gained into the relevance of this phenomenon to the study of biological systems by considering the case of dielectric particles suspended in electrolytic solutions. A mathematical treatment will be presented in section 3.3.3. Next, we focus our attention on the application of a model for stacked dielectric layers to probing the molecular organization of bilayer lipid membranes.

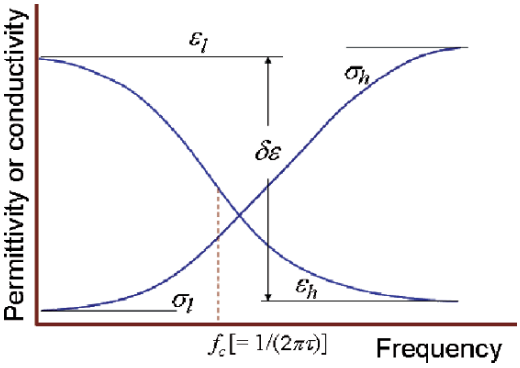

Fig. 3.7 Real [equation (3.42)] and imaginary [equation (3.4)] parts of the Debye dispersion function [equation (3.41)] and their parameterization.

3.3.2.2 The Dielectric Structure of Synthetic Lipid Bilayers and Plasma Membranes

It is possible to create experimentally bilayer lipid membranes that fill a small orifice in a slab of solid material immersed in an electrolyte, and to study the properties of the bilayer. Even before the fluid mosaic model of the membrane has been proposed (Singer and Nicolson, 1972), several researchers have used this method to study the dielectric behaviour of lipid bilayers as a function of the frequency of an alternating field applied between two electrodes each located on one side of the membrane (see, e.g., Ashcroft et al., 1981; White, 1973).

We will show here that, by using the lipid bilayer as a model for natural membranes and by regarding it as a dielectric multilayer, it is possible to validate the structural aspect of the Singer-Nicolson model by comparing its predicted dispersion curves to the experimental data. In doing so, we take into account not only the layered structure of the bilayer itself, but also an electrical *double layer capacitance* for each side of the *lipid bilayer*, as given by equation (3.27). This membrane model and its equivalent electrical circuit is shown in Fig. 3.8. By using this dielectric model, one can derive a formula for the real part of the admittance of the membrane (i.e., for equivalent conductance, G) and one for the imaginary part of the admittance divided by the frequency (which provides the equivalent capacitance, C), in terms of the specific electrical properties of each dielectric layer.

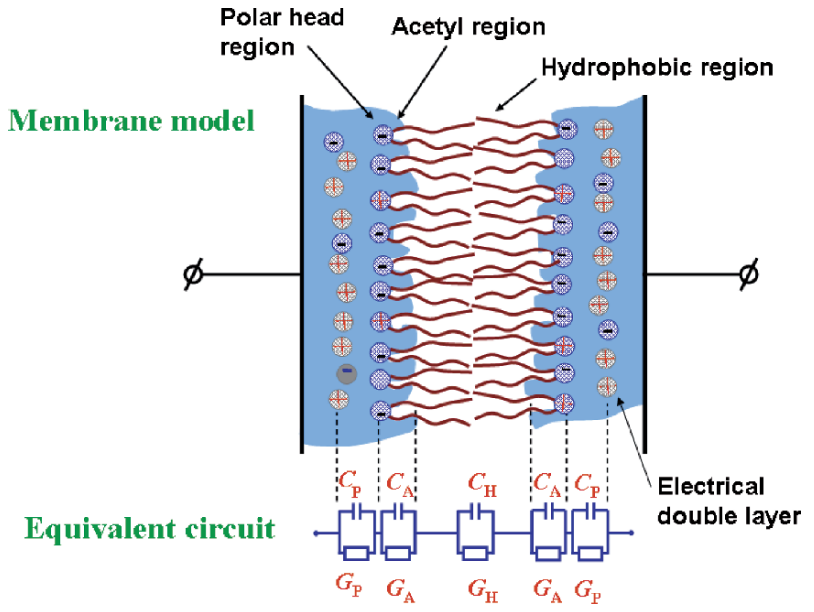

Fig. 3.8 Structural model of a bilayer lipid membrane placed in an electrolytic solution and its equivalent electrical circuit. Note that each lipid monolayer contributes an identical group of capacitance and conductance. C_P, C_A and C_H represent the capacitances, and G_P, G_A and G_H represent the conductances of the membrane layers.

Ashcroft and co-authors (1981) have performed measurements of capacitance and conductance of lipid bilayers (made from egg phosphatidyl-choline dissolved in *n*-tetradecane or *n*-decane solvents) in aqueous electrolyte solutions of KCl with various concentrations ranging from 1 to 1,000 mM. The results of their measurement of the electrical capacitance for the case of phosphatidyl-choline/tetradecane bilayer in 1 mM KCl solution are shown in Fig. 3.9, together with the curve predicted by the model from Fig. 3.8.

Quiz 2. Derive expressions for the equivalent conductance and capacitance of the model membrane presented in Fig. 3.8. Use equation (3.33) to express the admittance of each dielectric layer in terms of its specific conductance and capacitance.

To test the dielectric model of the lipid membrane, Ashcroft et al. have adjusted the C and G values corresponding to each dielectric layer until the simulated capacitance curve (represented by lines in Fig. 3.9) accurately fitted the data (represented by filled circles or triangles). These *best-fit values* have then been taken as the actual electrical properties of each particular layer. (Conductance dispersion curve and conductances for each layer have also been obtained by Ashcroft et al., but these are not very relevant to our discussion here.)

The specific capacitances of each dielectric layer for the membrane for bilayers immersed in 10 mM KCl solution were: $43\,\mu F/cm^2$ for the polar head layer (which includes the electrical double layer), $45\,\mu F/cm^2$ for the acetyl region layer, and $0.54\,\mu F/cm^2$ for the hydrophobic layer. (Note that these values include a factor of two that comes from the double layered structure of the membrane). Of these three values, most important for our discussion here are the first value, which compares well to what is expected ($\sim 100\,\mu F/cm^2$) from electrical double layer considerations

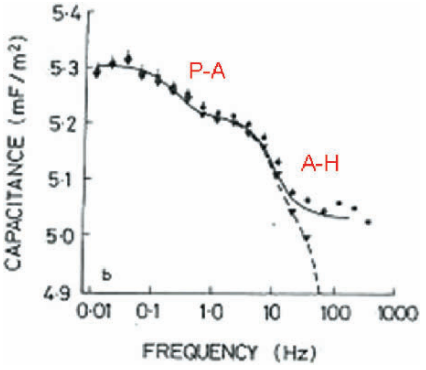

Fig. 3.9 Specific electrical capacitance of a model lipid bilayer in 1 mM aqueous KCl solution as a function of frequency of an applied electrical field. Points, experimental data; lines, simulations by using the model in Fig. 3.8. The filled circles and the solid line represent the data for the bilayer alone, while the dashed line and the triangles include uncorrected contribution from the bulk electrolyte. Note that there are two interfaces for each lipid monolayer, viz., one between the polar head layer and electrolyte and one between the hydrophobic layer and the acetyl layer, each of which contributes one dispersion (for a total of two sub-dispersions) represented by "P-A" and "A-H," respectively. (Figure adapted from Ashcroft et al., 1981).

(see section 3.2), and the one obtained for the hydrophobic layer. The latter, can be used to estimate the thickness of the hydrophobic layer (by using a value of 2.1 for the relative dielectric constant of that layer), which turns out to have a thickness of 3.5 nm. This value is very close to the one obtained by Fricke for the plasma membrane (mentioned in section 3.1.) from measurements in the radiofrequency range (Fricke, 1927) of plasma membrane, and for very good reasons.

To be meticulous, however, we should remark that slightly larger values $(0.73\,\mu F/cm^2)$ have been obtained for the specific capacitance of the hydrophobic layer (Benz and Janko, 1976) in the case of bilayers that contained no dissolved solvent (alcohol) in their hydrophobic core (so-called *black lipid bilayers*). In this case, the membrane thickness is slightly smaller, since only the lipid tails are occupying now the hydrophobic layer volume.

3.3.3 Dielectric Properties of Random Suspensions of Particles with Particular Relevance to Biological Cells

Specific capacitance of the plasma membrane can be measured for instance by using micropipette techniques, in which portions of the membrane are attached to the tip of a micropipette and subjected to an applied electrical field (see, e.g., Asami and Takashima, 1994). However, to determine the dielectric properties of biological cells in a completely noninvasive manner, one typically performs measurements on suspensions.

Dielectric properties of systems of microscopic particles depend on a number of physical as well as geometrical factors:

1. Electrical properties of the particles and the suspending medium (see below)
2. The particles concentration (see below)
3. The particle shape (Takashima, 1989)
4. Whether or not the particle has a peculiar structure (i.e., it is itself heterogeneous, see below)
5. Whether the particles are individually dispersed to form random suspensions (Raicu et al., 1996, 1998a) or more orderly aggregates (Raicu et al., 1998b, 2001)

In this regard, one distinguishes three types of aggregates: (a) dilute random suspensions of particle aggregates; (b) concentrated suspensions of aggregates; and (c) large, self-similar aggregates, such as percolation and *Cantorian fractals* (see chapter 5 for a discussion of fractals and fractal structures in biophysics).

In this book we are only interested in the rather simple theory of Maxwell-Wagner relaxation as it applies to the plasma membrane.

3.3.3.1 Homogeneous Particles in Applied Homogeneous Electrical Field

In order to determine the equivalent dielectric constant of a suspension, one has to calculate, by solving the Laplace equation (Jackson, 1998) the electric potential at a

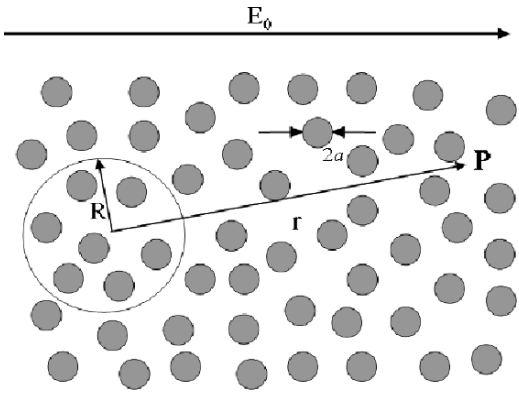

Fig. 3.10 The geometry parameters necessary for the determination of the potential of a suspension of spherules of radius a (at a point, P, within the suspension). The complex permittivity, ε_s^*, is assumed to be distributed at random in a uniform medium of complex permittivity, ε_e^*.

point, P, due to a spherule of radius a placed in an electrical field, E_0. Then, a region in space, containing n spherules, delimitated by an imaginary sphere of radius, R, is considered as having dielectric properties similar to the whole suspension of interest (Fig. 3.10). The distances from each spherule to the point, P, are considered so large that the spherules can be regarded as being all located at the same distance r from the point P. The potential is then obtained as a superposition of all the potentials calculated for each spherule (Hanai, 1960; Takashima, 1989):

$$\Phi(r,\theta) = -E_0 r \cdot \cos\theta + n\frac{a^3}{r^2} \cdot \frac{\varepsilon_s^* - \varepsilon_e^*}{\varepsilon_s^* + 2\varepsilon_e^*} E_0 \cos\theta. \tag{3.44}$$

where n is the number of particles and θ represents the angle between $\vec{E}_0$ and $\vec{r}$.

Next, the potential due to the large sphere of radius, R, assumed to be homogeneous and having the complex permittivity, ε^*, is obtained as:

$$\Phi(r,\theta) = -E_0 r \cdot \cos\theta + \frac{R^3}{r^2} \cdot \frac{\varepsilon^* - \varepsilon_e^*}{\varepsilon^* + 2\varepsilon_e^*} E_0 \cos\theta. \tag{3.45}$$

Since the potentials determined by the two methods should be equal (they characterize the same system), we obtain:

$$\frac{\varepsilon^* - \varepsilon_e^*}{\varepsilon^* + 2\varepsilon_e^*} = p \cdot \frac{\varepsilon_s^* - \varepsilon_e^*}{\varepsilon_s^* + 2\varepsilon_e^*} \tag{3.46}$$

where $p = n\frac{a^3}{R^3}$ is the *volume fraction* of the suspended particles.

Upon some algebraic manipulation of equation (3.46), an equation formally equivalent to the Debye equation (see equation 3.41) is obtained for the equivalent complex permittivity of the suspension, ε^* (Hanai, 1960).

3.3.3.2 Particles Covered by a Thin Membrane: The Single-Shell Model

Mile and Robertson (1932) made use of the classical potential theory and calculated the potential outside of a shelled sphere suspended in a medium of permittivity ε_e^* as:

$$\Phi(r,\theta) = -E_0 r \cdot \cos\theta + n\frac{R^3}{r^2} \cdot \frac{(\varepsilon_m^* - \varepsilon_e^*)(\varepsilon_i^* + 2\varepsilon_m^*) + (\varepsilon_i^* - \varepsilon_m^*)(\varepsilon_e^* + 2\varepsilon_m^*)v}{(\varepsilon_m^* + 2\varepsilon_e^*)(\varepsilon_i^* + 2\varepsilon_m^*) + 2(\varepsilon_i^* - \varepsilon_m^*)(\varepsilon_e^* - \varepsilon_m^*)v} E_0 \cos\theta, \tag{3.47}$$

where ε_e^*, ε_i^*, ε_m^* represent the complex permittivities of the layers in Fig. 3.11. The equation for permittivity, obtained from equality of this potential to the one given by equation (3.45), is:

$$\frac{\varepsilon^* - \varepsilon_e^*}{\varepsilon^* + 2\varepsilon_e^*} = p \cdot \frac{(\varepsilon_m^* - \varepsilon_e^*)(\varepsilon_i^* + 2\varepsilon_m^*) + (\varepsilon_i^* - \varepsilon_m^*)(\varepsilon_e^* + 2\varepsilon_m^*)v}{(\varepsilon_m^* + 2\varepsilon_e^*)(\varepsilon_i^* + 2\varepsilon_m^*) + 2(\varepsilon_i^* - \varepsilon_m^*)(\varepsilon_e^* - \varepsilon_m^*)v}, \tag{3.48}$$

where $p = na^3/{R_c}^3$ and $v = (R_c - d)^3/{R_c}^3$ (see Fig. 3.11). This equation is sometimes improperly attributed to Pauly and Schwan (1959).

Dänzer (1993) and, later, Pauly and Schwan (1959) have undertaken detailed analyses of the equation for shelled spheres (equation 3.48) and found after somewhat cumbersome calculations that it is exactly decomposable into two terms of a Debye type, corresponding to the two interfaces of the particles.

Fricke (1955) had generalized the Mile and Robertson model to include multi-shelled particles, and obtained an equivalent admittance of the form of a continued fraction. Later, Irimajiri et al. (1979) have shown that a number of sub-dispersions equal to the number of interfaces should be expected for multi-shelled particle suspensions. For single-shelled particles, therefore, two sub-dispersions are expected to occur, but usually only one sub-dispersion is important – the one due to the polarization at the interface between the suspending medium and cell membrane. Pauly and Schwan (1959) have derived this result by considering the following reasonable approximations:

$$\frac{\sigma_m}{\sigma_e}, \frac{\sigma_m}{\sigma_i}, \frac{d}{R} \ll 1, \tag{3.49}$$

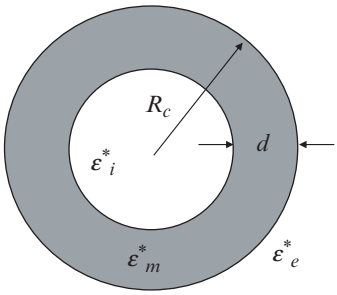

Fig. 3.11 The *single-shell dielectric model* of a particle covered with a thin shell.

which state that the cell membrane is insulating, compared to the internal and external electrolytes, and very thin. Thus, the parameters for the equivalent Debye equation are:

$$\sigma_l = \sigma_e \frac{2(1-p)}{2+p} \tag{3.50}$$

$$\delta\varepsilon \equiv \varepsilon_l - \varepsilon_h = \frac{9p}{(2+p)^2} \frac{RC_m}{\varepsilon_0} \tag{3.51}$$

$$\tau \equiv \frac{1}{2\pi f_c} = RC_m \left(\frac{1}{\sigma_i} + \frac{1-p}{2+p} \frac{1}{\sigma_e} \right), \tag{3.52}$$

where C_m is the specific plasma membrane capacitance, defined as

$$C_m = \frac{\text{Membrane capacitance}}{\text{Surface area}} \equiv \frac{\varepsilon_m}{d}. \tag{3.53}$$

C_m can be easily obtained from equation (3.52), upon knowledge of the volume fraction, p (derived from 3.50).

By performing dielectric measurements on suspensions of cells, it has been possible to determine the specific electrical capacitance of the plasma membrane for many different types of biological cells. For instance, a value of $0.72\,\mu\text{F/cm}^2$ has been obtained for erythrocyte ghosts (Asami et al., 1989), while for yeast cells values between 0.65–$0.75\,\mu\text{F/cm}^2$ have been reported (Raicu et al., 1996, 1998a).

For a better understanding of those results, in which a constant membrane capacitance is obtained at all frequencies above kHz-region, it is necessary to discuss them in light of the results presented above for lipid bilayers. Specifically, it was observed that the dielectric dispersion of the membrane itself takes place at low frequencies. After 1 kHz, the only contribution to the membrane capacitance is due to the hydrophobic layer alone; this is therefore the contribution that was expected to be obtained from measurements of cells in suspension, which are carried out at frequencies above 1 kHz. Therefore, one can conclude that the capacitance of biological cell membrane, measured in radiofrequency range provides a value for the thickness of the hydrophobic layer of the order of 3–4 nm, which supports the current membrane model, in particular the fact that a lipid bilayer provides a matrix for all membrane components.

References

Asami, K. and Takashima, S. (1994) Membrane admittance of cloned muscle cells in culture: use of a micropipette technique, *Biochim. Biophys. Acta*, **1190**: 129

Asami, K., Takahashi, T. and Takashima, S. (1989) Dielectric properties of mouse lymphocytes and erytrocytes, *Biochim. Biophys. Acta*, **1010**: 49

Ashcroft, R. G., Coster, H. G. L. and Smith, J. R. (1981) The molecular organisation of bimolecular lipid membranes. The dielectric structure of the hydrophilic/hydrophobic interface, *Biochim. Biophys. Acta*, **643**: 191

Atkins P. and de Paula J. (2002) *Atkins' Physical Chemistry*, 7th ed., Oxford University Press, New York

Berg, J. M., Tymoczo, J. L. and Stryer, L. (2002) *Biochemistry*, 5th ed., W. H. Freeman, New York

Brett, C. M. A. and Oliveira Brett, A. M. (1993) *Electrochemistry. Principles, Methods, and Applications*, Oxford University Press, Oxford/New York/Tokyo

Benz, R. and K. Janko (1976) Voltage-induced capacitance relaxation of lipid bilayer membranes. Effects of membrane composition, *Biochim. Biophys. Acta*, **455**: 721

Dänzer, H. (1938) In: E. B. Rajewsky (ed.) *Ergebnisse der Biophysikalischen Forschung*, Georg Thieme, Leipzig, p. 193

Debye, P. (1945) *Polar Molecules*, Dover, New York

Fricke, H. (1927) The electric capacity of suspensions of red corpuscles of a dog, *Phys. Rev*., **26**: 682

Fricke, H. (1955) The complex conductivity of a suspension of stratified particles of spherical cylindrical form, *J. Phys. Chem*., **59**: 168

Frye, C. D. and Edidin, M. (1970) The rapid intermixing of cell surface antigens after formation of mouse-human heterokaryons, *J. Cell. Sci*., **7**: 319

Glaser, R. (2001) *Biophysics*, Springer, Berlin/Heidelberg/New York

Goodwin, J. S., Drake, K. R., Remmert, C. L. and Kenworthy, A. K. (2005) Ras diffusion is sensitive to plasma membrane viscosity, *Biophys. J*., **89** (2): 1398

Hanai, T. (1960) Theory of the dielectric dispersion due to the interfacial polarization and its application to emulsions, *Kolloid. Z.* **171**: 3

Hille, B. (2001) *Ion Channels of Excitable Membranes*, Sinauer, Sunderland, MA

Hunter, R. J. (1987) *Foundations of Colloid Science*, Vol. 1, Oxford University Press, Oxford

Irimajiri A., Hanai T. and Inouye H. (1979), A dielectric theory of 'multi-stratified shell' model with its application to a lymphoma cell, *J. Theor. Biol*., **78**: 251

Jackson, J. D. (1998) *Classical Electrodynamics*, Wiley, New York, p. 154

Lodish, H., Berk, A., Matsudaira, P., Kaiser, C. K., Krieger, M., Scott, M. P., Zipursky, S. L. and Darnell, J. (2004) *Molecular Cell Biology*, 5th ed., W. H. Freeman, New York

Mile, J. B. and Robertson, H. P. (1932) By assuming the material to be made up of elements of different relaxation times, interface may play a large role during the formation of a field-induced dipole moment, *Phys. Rev*., **40**: 583

Movileanu, L., Popescu, D., Stelian, I. and Popescu, A. I. (2006) Transbilayer pores induced by thickness fluctuations, *Bull. Math. Biol*. **68**: 1231

Pauly, H. and Schwan, H. P. (1959) Über die Impedanz einer von kugelförmigenTeichen mit eine Schale *Z. Naturforsch*., **14b**: 125

Popescu, D., Ion, S., Popescu, A. and Movileanu, L. (2003) Elastic properties of BLMs and pore formation, In: *Planar Lipid Bilayers (BLMs) and Their Applications*, Tien, H.T. and Ottova-Leitmannova, A. (Eds.), Elsevier Science, Amsterdam/New York, Chapter 5, p. 173

Raicu, V., Raicu, G. and Turcu, G. (1996) Dielectric properties of yeast cells as simulated by the two-shell model, *Biochim. Biophys. Acta*, **1274**: 143

Raicu, V., Gusbeth, C., Anghel, D. F. and Turcu, G. (1998a) Effects of cetyltrimethylammoniumbromide (CTAB) surfactant upon the dielectric properties of yeast cells, *Biochim. Biophys. Acta*, **1379**: 7

Raicu, V., Saibara, T. and Irimajiri, A. (1998b) Dielectric properties of rat liver in vivo: Analysis by modeling hepatocytes in the tissue architecture, *Bioelectrochem. Bioenerg*., **47**: 333

Raicu, V., Sato, T. and Raicu, G. (2001) Non-Debye dielectric relaxation in biological structures arises from their fractal nature, *Phys. Rev. E*, **64**: 02191

Singer, S. J. and Nicolson, G. L. (1972) The fluid mosaic model of the structure of cell membranes, *Science*, **175**: 720

Stern, O (1924) Zur Theorie der Electrolytischen Doppelschicht, Z. Elektrochem., **30**: 508

Takashima, S. (1989) *Electrical Properties of Biopolymers and Cell Membranes*, Adam Hilger, Bristol

White, S. H. (1973) The surface charge and double layers of thin lipid films formed from neutral lipids, *Biochim. Biophys. Acta* **323**: 343